

BIOPHOTONICS

DOI: 10.1070/QEL15930

Capabilities of laser technology for manufacturing diagnostic peptide matrices with maximal density

O.I. Baum, E.M. Shcherbakov, A. Nesterov-Müller, E.N. Sobol'

Abstract. **The process of manufacturing a matrix-gel biochip is modelled by means of laser fused deposition of a layer of polymer microparticles, containing a sensitive peptide element, onto a glass substrate. The limits of acceptable ranges and the optimal values of laser parameters, at which the melting of the polymer coating occurs without damaging the sensitive elements of the biochip, are theoretically determined. The results of the experiments on laser fused deposition of a layer of microparticles having the size 3–4 μm confirm the conservation of the functions of the biological complexes at optimal irradiation regimes. The parameters of the laser impact affecting the possible minimal separation between the zones of laser fused deposition are investigated. The essential role of heat conductivity and thermoplasticity of the polymer in increasing the size of the melted droplet is demonstrated. Using the laser radiation with the wavelength 532 nm focused into a spot with the diameter 6 μm (the laser pulse duration being 10 ms) the laser fused deposition density of 110000 spots per 1 cm^2 is achieved. The maximal estimated density of laser fused deposition for the studied system amounts to 250000 spots per 1 cm^2.**

Keywords: *laser, biochip, diagnostic peptide matrices, laser fused deposition, heat conductivity, thermoplasticity.*

1. Introduction

The necessity to carry out a large number of analyses and similar-type examinations with a small amount of material has led to the invention of biochips that allow parallel and simultaneous execution of several tests and joining a variety of analogous test systems in one carrier [1]. A biochip consists of a substrate, on which at definite places the sensitive elements, capable of reacting with the compounds of the studied sample are deposited.

At present, there are three main types of biochips, namely, cell, protein and DNA biochips. For the first time the binding of cells to the immobilised antibodies on a biochip was implemented by Chang [2]. In 2000 MacBeath and Schreiber [3] created the first protein biochip. A set of different DNAs joined into a biochip was created in 1987 and applied to determine the specific features of the regulation of gene expression by interferons [4], and the complete eukaryotic genome was disposed on a microchip as soon as in 1997 [5].

The existing microchips can be divided into two classes [6], namely, the micromatrices of different compounds, mainly biopolymers, immobilised on the substrate surface, and the miniaturised microlaboratories. The essential contribution to the development of microchips was made by Mirzabekov [7–9] and Ekins [10–12], who have shown that the dimensions of the analytic system in the immunology can be reduced without the loss of sensitivity. The creation of DNA biochips appeared to be a much simpler problem than that of the protein biochips, since the DNA molecules do not differ strongly from each other from the point of view of biochemistry and biophysics and are more stable. On the contrary, the proteins differ strongly in their biochemical properties, which gives rise to the problem of binding the same quantity of different proteins on one substrate. Moreover, some proteins require specific substrates [13]. The additional difficulty follows from the fact that in the course of immobilisation the structure of a protein can change. Thus, the main problem in biochip manufacturing is the compactness of the arrangement of the sensitive complexes of the substrate. At present for the DNA biochips the density achieves ~400000 spots per 1 cm^2, while for the protein biochips in most cases the density does not exceed 1000 sensitive complexes per the same area.

Now there are two main technologies of biochip fabrication. 1. For the matrix biochips, the necessary proteins are distributed over the sectors of a specially selected substrate. The binding to the substrate is usually implemented by heating (accompanied by the diffusion of the antibody from the coating into the substrate) or adsorption. 2. For gel biochips the gel droplets are deposited above the coating, and in these droplets the antibodies are immobilised. The advantages of this technology are the greater safety of antibodies in the gel and the possibility of introducing the quantity of antibodies greater by an order of magnitude, as well as the use of large specific biostructures. However, all this leads to larger element size, slower kinetics and more complicated analysis, as compared to the matrix biochips.

Both technologies possess mutual problems, namely, the large dimensions and excess number of antibodies, which essentially increases the biochip cost. The problem can be solved using the spot laser fused deposition, the study of which is the aim of the present paper. The urgency of the problem is caused by the fact that the diagnostics (particularly, the early diagnostics) of the immune system diseases

O.I. Baum, E.M. Shcherbakov, E.N. Sobol' Institute on Laser and Information Technologies, Russian Academy of Sciences, ul. Pionerskaya 2, Troitsk, 142190 Moscow, Russia; e-mail: baumolga@gmail.com, jenya_sh89@mail.ru, esobol@rambler.ru; **A. Nesterov-Müller** Karlsruhe Institute of Technology Institute of Microstructure Technology, Hermann-von-Helmholtz-Platz 1D-76344 Eggenstein-Leopoldshafen, Germany; e-mail: alexander.nesterov-mueller@kit.edu

Received 4 September 2015; revision received 18 November 2015
Kvantovaya Elektronika **46** (2) 173–178 (2016)
Translated by V.L. Derbov

and the type of neoplasms of biotissues in the course of their regeneration [14] remain to be among the most important problems of medicine. For their solution, one can successfully use the peptide matrices interacting with the biological tissues. Unfortunately, the creation of peptide high-density libraries remains to be an unsolved problem.

The presents work is based on the generalised matrix-gel technology [15], in which the immobilisation of sensitive elements, enclosed in a special polymer shell, is implemented using the spot laser fused deposition.

Earlier in our paper [16] the impact of the laser radiation with the wavelength 810 nm on a similar system was considered and the power densities were determined that provided the shell melting, but did not damage the sensitivity element. The safety of the latter was studied and confirmed experimentally using the methods of thermometry, luminescence and Raman spectroscopy. However, the characteristics of laser radiation used in Ref. [16] did not allow the focusing of radiation into a spot with the diameter smaller than 30 μm, so that the density of deposited elements was not high.

In the present work, we use the potassium titanyl phosphate crystal laser Ventus VIS (Laser Quantum LTD) with the radiation wavelength 532 nm that allows a smaller diameter of the beam spot and, therefore, a larger area density of deposited elements. We study the possibility of creating a biochip by laser heating of a layer of spherical polymer microparticles with the sensitive element inside each to the stage of the polymer shell melting. We reveal the heating parameters, such that the shell is melted, but the sensitive element is not damaged. The situation of laser impact with a larger beam spot (the spot diameter being comparable with the thickness of the polymer film) is theoretically considered and the experiments proving the conservation of functions of the biological complexes under the found parameters of irradiation at the wavelength of 532 nm are carried out. To increase the density of the spot laser fused deposition, we proceed to the impact with the small laser spot diameter, comparable with the diameter of the polymer microparticles. The parameters affecting the possible minimal separation between the spots of the laser impact and the role of the plasticity in increasing the size of the melted droplets are studied. Finally, we determine the maximal possible density of elements on the substrate.

2. Materials and methods

The object of the study was a porous three-component medium on a glass substrate, consisting of polystyrene polymer spheres with the radius 3–4 μm (88% of the total medium volume), in which the sensitive element biotin-pentafluorophenyl-ester (10%) was contained together with the graphite nanoparticles (2%) intended to increase the absorption coefficient of the medium.

The irradiation leading to the polymer melting and formation of spot droplets on the substrate was implemented using the Ventus VIS laser (Laser Quantum LTD) with the radiation wavelength 532 nm. The parameters of the impact were chosen within the acceptable range, the limits of which were found by means of theoretical modelling. The laser melting of the polymer shell released the sensitive bioelements for subsequent impregnation into the surface layer of the substrate with the given spatial distribution and density during the characteristic heating times chosen to leave them undamaged.

To study the safety of the sensitive element after the laser impact, a layer of luminophore streptavidin alexa fluor 546 (Life Technologies Corporation) was deposited on the substrate that chemically reacted with the sensitive element, if the biological and chemical activity of the latter was preserved. Then using a GenePix 4000B Microarray Scaner (Molecular Devices, LLC) the luminescence was observed, the presence of which was an evidence of the saved activity of the sensitive elements.

3. Theoretical description of the process of laser melting of the three-component medium without damaging the biochip sensitive elements

To determine the acceptable regimes of laser impact let us consider the possible mechanisms of the sensitive element destruction in the course of laser melting of the polymer matrix on the substrate.

3.1. Thermal destruction leading to the sensitive element melting

To find the temperature distribution in the film–substrate system we considered the heat conduction problem for the heat propagation through a porous three-component semispace, forming a thin film of the glass substrate. In the first approximation, the material irradiated by the laser beam was assumed isotropic, and the optical and thermal physical coefficients were assumed independent of temperature. The concentration of graphite, the basic absorbing agent in the system, was assumed uniform. In the case of sufficiently thin (less than 7 μm) deposited films the high temperature conductivity of graphite provided their uniform heating over the thickness. For the laser beam diameter 15 μm significantly exceeding the film thickness one can consider a one-dimensional problem of heating a thin film on a substrate, assuming that the absorbability of the film is a function of its thickness and all the energy absorbed in the film is released uniformly over its thickness. These assumptions in the first approximation allowed us to use the analytical solution of the heat conduction problem in the form [17]:

$$T(t) = \frac{q\sqrt{a_2 t}}{\lambda_2}\left[\frac{2}{\sqrt{\pi}} + \psi\left(\exp\frac{1}{\psi^2}\operatorname{erfc}\frac{1}{\psi} - 1\right)\right], \qquad (1)$$

where a_1, a_2 is the temperature conductivity; c_1, c_2 is the heat capacity; $\psi = c_1 h/(c_2\sqrt{a_2 t})$ (the subscripts 1 and 2 refer to the film and the substrate, respectively); q is the power density; h is the thickness of the layer of microparticles on the substrate; and λ_2 is the heat conductivity coefficient of the substrate. The total amount of heat, passing through the area S during the time of laser heating τ and expressed in terms of the heat flow density q', heats the volume V depending on the heat propagation depth $\sqrt{a_2\tau}$:

$$q'S\tau == c_2\Delta TV = c_2 \operatorname{grad} T(h + \sqrt{a_2\tau})S.$$

If the film of microparticles is considered to be thin, i.e., $h \ll \sqrt{a_1\tau}$, then the maximal temperature at its surface is found from expression (1) as

$$T_{\max} = \frac{2q\sqrt{a_2\tau}}{\lambda_2\sqrt{\pi}}. \qquad (2)$$

If the sensitive element is destroyed at the definite temperature T^*, then formula (2) allows the determination of the dependence of the threshold power of the laser radiation on the duration of the impact.

3.2. Thermomechanical destruction of the sensitive element

The second possible mechanism of destructing the sensitive element is due to the appearance of thermomechanical stresses under the inhomogeneous laser heating. In correspondence with the thermoelasticity theory [18] the temperature gradients arising under the laser impact cause the stresses

$$\sigma_r = \frac{\alpha E T_{max}}{1-2\nu} = \frac{\alpha E}{1-2\nu}\frac{2q\sqrt{a_2\tau}}{\lambda_2\sqrt{\pi}},$$

where α is the coefficient of thermal expansion; E is the elasticity modulus, and ν is the Poisson coefficient. It is assumed, that the destruction of the sensitive peptide occurs if the stress achieves the ultimate strength σ_r. This mechanism of destruction occurs in the region of laser parameters that can intersect with the region of thermal destruction, thus limiting the desired impact range. For the power density leading to the peptide destruction we obtain

$$q_r = \frac{\sigma_r \lambda_2 (1-2\nu)\sqrt{\pi}}{2\alpha E\sqrt{a_2\tau}}. \quad (3)$$

The calculations performed with the help of the theoretical model allowing the determination of the temperature field in the film-substrate system yielded the range of laser parameters for which the laser heating of the layer of polymer microparticles containing a sensitive element leads to the melting of the polymer shell, keeping unchanged the functional capability of the sensitive element.

Substituting into Eqn (1) the temperature that corresponds to the beginning of the melting process (70 °C) and the maximal temperature at which the functional capability [19] of the biological biotin-pentafluorophenyl-ester complex is conserved (90 °C) for the exposure duration of 10 ms, we obtained the range of power densities, in which the outer polymer shell of the microparticles is melted without damaging the sensitive elements inside them. This range amounts to 25–35 W cm^{-2}.

The results of calculating the boundaries of the acceptable laser influence regimes using Eqns (2) and (3) are presented in Fig. 1. Curve (*1*) corresponds to the beginning of the polymer shell melting process heated from the room temperature (20 °C). One can see that for the lower boundary of the power density 25 W cm^{-2} chosen for further experiments the melting begins after heating during 10 ms. Curve (*2*) corresponds to the beginning of thermal destruction of the sensitive element. For the upper boundary of the power density 35 W cm^{-2} chosen for our experiments the process begins after 10 ms of heating. Curve (*3*) corresponds to the power density, for which the destruction of the sensitive element occurs due to the expansion–compression stresses, calculated using formula (3) ($\sigma_r = 40$ MPa, $\lambda_2 = 1$ W (m K)$^{-1}$, $\nu = 0.35$, $\alpha = 70\times10^{-6}$ K^{-1}, $E = 1.2$ GPa, $a_2 = 3.4\times10^{-7}$ m^2 s^{-1} [20]). For the considered case at the 10th millisecond of heating it amounts to 32.5 W cm^{-2}, which limits the range of possible power densities from above. Thus, the optimal region for minimising the melted spot radius is the region between curves (*1*, *2*) below curve (*3*) in Fig. 1.

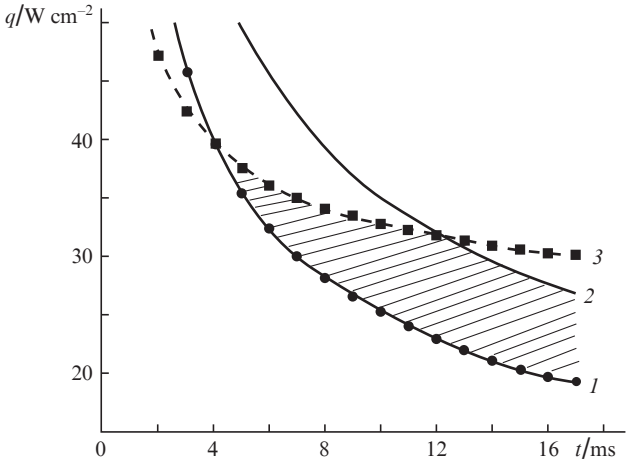

Figure 1. Boundaries of the zone of acceptable regimes of laser impact for the laser fused deposition of a thin film of sensitive elements, coated with a polymer shell: the beginning of the process of melting of the polymer shell under the heating from the temperature 20 °C (*1*); the beginning of the thermal destruction of the sensitive element (*2*); and the power density, for which the destruction of the sensitive element occurs due to the extension-compression stresses in the irradiated system (*3*). The zone of acceptable regimes is shaded.

4. Experimental study of the processes of laser fused deposition of sensitive peptides in polymer shells onto the glass substrate

4.1. Effect of laser parameters on the fused droplet size

We studied the effect of the laser radiation parameters on the value of the area subjected to the laser impact. The mean power of the radiation varied from 150 mW to 330 mW, and the pulse duration from 5 to 14 ms. The diameter of the laser spot on the substrate surface with polymer film amounted to 15 μm and the separation between the centres of laser impact was 100 μm. The minimal size of the fused polymer droplets in these experiments was 30 μm.

To study the safety of the functional capability of the sensitive element after the laser impact, the substrate was coated with a layer of luminophore that chemically reacted with the sensitive element if the latter saved its biological and chemical activity. The presence of the luminescence confirmed the conservation of the sensitive elements activity (Fig. 2).

4.2. Fused deposition in the case of small laser spot diameter

We performed the polymer fused deposition onto the substrate in the regime, close to that with the optimal parameters, namely, the laser radiation wavelength 532 nm, the power 40 mW and the processing time 10 ms. The radiation was supplied through an optical fibre with the diameter 600 μm with subsequent focusing into a spot with a diameter 6 μm. Figure 3 presents an optical photograph of the fused droplets with the mean diameter 13.5 ± 0.5 μm, the polymer film grain size being 3–4 μm.

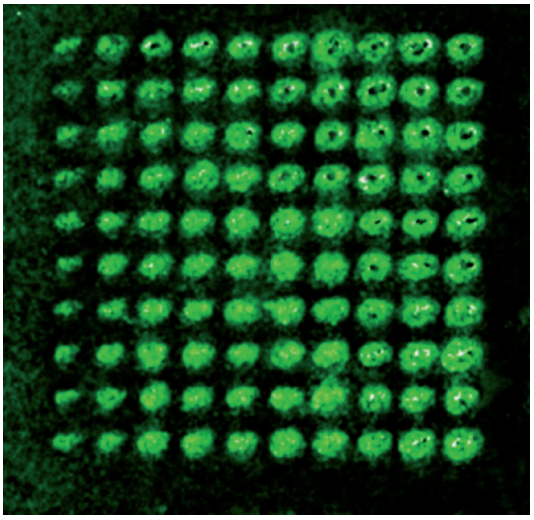

Figure 2. Droplets of melted polymer with sensitive elements inside, processed with the streptavidin alexa fluor 546 luminophore. The power of laser radiation varied from 150 to 330 mW from bottom to top with the step 20 mW, the pulse duration varied from 5 to 14 from left to right with the step 1 ms.

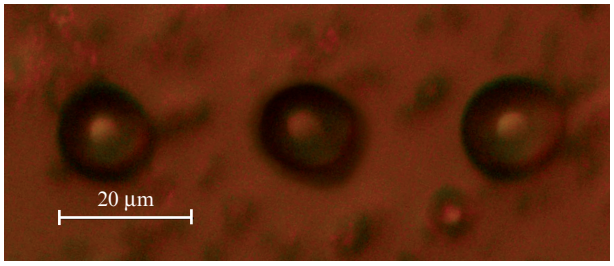

Figure 3. Optical photograph of welded polymer drops.

5. Estimate of the maximal deposition density

The deposition density is limited by the minimal size L of the spot of laser effect, which is a sum of the laser spot diameter d and the heated zone dimension:

$$L = d + 2\sqrt{a_1\tau}\,.$$

Thus, one can calculate the minimal separation between the laser impact centres, and their maximal density can be determined as

$$\frac{1}{L^2} = \frac{1}{(d + 2\sqrt{a_1\tau})^2}. \tag{4}$$

For the considered system (Fig. 2) the maximal deposition density, calculated using formula (4) with the laser beam diameter 15 μm, was 30000 spots per 1 cm^2. The reduction of the spot diameter by two times did not lead to the increase of the density of the chip sensitive elements by four times. The diameter of the laser impact zone and the maximal density of deposition are essentially affected by plasticity of the material that arises under the inhomogeneous heating beyond the melting zone.

6. Effect of thermoplasticity on the maximal deposition density

To determine the region of parameters in which the thermoplasticity is observed, in the thermoelasticity theoretical model [18] the approximation of a thin film in the temperature field $T(r, q, \tau)$ is used and the system of differential equations of equilibrium is solved without considering the distributed surface load. We assume that the stresses and the displacements caused by the heating do not change within the thin plate over its thickness. The radial and the angular stresses, σ_r and σ_θ, must satisfy the equilibrium equation

$$\frac{d\sigma_r}{dr} + \frac{\sigma_r - \sigma_\theta}{r} = 0. \tag{5}$$

Let us denote by ε_r the total radial deformation and by $\varepsilon_r - \alpha T(r, q, \tau)$ its part due to the thermal stress. Then for the radial and angular component of the deformation in the polar coordinates we have

$$\begin{aligned} \varepsilon_r - \alpha T(r,q,\tau) &= \frac{1}{E}(\sigma_r - \nu\sigma_\theta), \\ \varepsilon_\theta - \alpha T(r,q,\tau) &= \frac{1}{E}(\sigma_\theta - \nu\sigma_r). \end{aligned} \tag{6}$$

Let us solve equations (5) and (6) with respect to the radial and angular stress components:

$$\begin{aligned} \sigma_r &= \frac{E}{1-\nu^2}[\varepsilon_r + \nu\varepsilon_\theta - (1+\nu)\alpha T(r,q,\tau)], \\ \sigma_\theta &= \frac{E}{1-\nu^2}[\varepsilon_\theta + \nu\varepsilon_r - (1+\nu)\alpha T(r,q,\tau)]. \end{aligned} \tag{7}$$

Substituting Eqns (7) into Eqn (5), we obtain:

$$r\frac{d}{dr}(\varepsilon_r + \nu\varepsilon_\theta) + (1-\nu)(\varepsilon_r - \varepsilon_\theta) = (1+\nu)\alpha r\frac{d[T(r,q,\tau)]}{dr}. \tag{8}$$

If we denote the radial displacement by u, then the radial and angular components of the deformation in the polar coordinates will have the form:

$$\varepsilon_r = \frac{du}{dr}, \quad \varepsilon_\theta = \frac{u}{r}.$$

Substituting these expressions into Eqn (8) and allowing for the fact that

$$u = (1+\nu)\alpha\frac{1}{r}\int_a^r T(r,q,\tau)r\,dr + C_1 r + \frac{C_2}{r},$$

we arrive at the final expressions for the stress components:

$$\begin{aligned} \sigma_r &= \alpha E\left[\frac{1}{b^2}\int_0^b T(r,q,\tau)r\,dr - \frac{1}{r^2}\int_0^r T(r,q,\tau)r\,dr\right], \\ \sigma_\theta &= \alpha E\left[-T(r,q,\tau) + \frac{1}{b^2}\int_0^b T(r,q,\tau)r\,dr + \frac{1}{r^2}\int_0^r T(r,q,\tau)r\,dr\right], \end{aligned} \tag{9}$$

where b is the limit of integration over the radius r.

The region of plastic deformations is determined by the von Mises criterion: $\sigma_\theta - \sigma_r = \sigma_s$, where σ_s is the stress component, corresponding to the yield stress leading to irreversible deformation [21]. The surface region with the radius r irradiated by the laser is not subject to destruction and expansion over the area, if the power of irradiation and its duration satisfy the inequality

$$\alpha E\left[\frac{2}{r^2}\int_0^r T(q,\tau,r)r\mathrm{d}r - T(q,\tau,r)\right] \leqslant \sigma_s. \quad (10)$$

In each layer, perpendicular to the direction of the laser beam propagation, the temperature can be approximated by the Gaussian distribution with the effective radius r_{eff}. In the polymer surface layer the maximum of temperature can be calculated from Eqn (2); then Eqn (1) can be written in the form

$$\alpha E\left[\frac{4}{r^2}\frac{q\sqrt{a_2\tau}}{\lambda\sqrt{\pi}}\int_0^r \exp\left(-\frac{r^2}{r_{eff}^2}\right)r\mathrm{d}r - \exp\left(-\frac{r^2}{r_{eff}^2}\right)\right] \leqslant \sigma_s. \quad (11)$$

Substituting into Eqn (11) the parameters, corresponding to the data of Fig. 3 [the power 40 mW, the time 10 ms, λ = 0.1 W (m K)$^{-1}$, $a_2 = 3.4\times10^{-7}$ m^2 s^{-1}], we obtain for the maximum of the left-hand side of Eqn (11) the value of 6.5 MPa, that satisfactorily agrees with the data on the yield stress in biopolymers σ_s = 12 MPa [14] and 7 MPa [22].

The calculations show that in this case the maximal stress is concentrated on the ring with the radius 13 μm. In this region, the polymer is melted along the ring, which leads to its fusion with the central spheroidal droplet at the expense of the capillary forces in the entire melted region, which increases the droplet radius and reduces the attainable density of laser fused deposition. The increase in the power and time of impact leads to an increase in the radius of the fused droplet. Thus, beyond the yield stress the diameter of the laser-deposited element grows, thus reducing the laser deposition density. The results of calculations by Eqn (1) show the essential contribution of thermoplasticity into the experimentally observed deviation of the dependence of the maximal density of the laser fused deposition on the laser spot diameter from the quadratic one.

7. Discussion

Theoretical modelling of various processes of damaging the sensitive element of the chip allowed the determination of the region of acceptable regimes (first of all, the intensity) of the laser impact. To increase the density of the deposited elements it is reasonable to decrease the diameter of the laser spot and the duration of the laser pulse to certain limits. For the laser pulses with the duration shorter than 4 ms the thermomechanical damage occurs at lower laser intensities than those required for the melting of the system. For the laser spot diameters smaller than 6 μm the minimal size of the melted region is largely dependent on the processes of heat transfer and the material thermoplasticity.

The experimental study of the influence of different parameters of laser irradiation on the size of the fused droplet confirmed the theoretical results and conclusions. In the left bottom part of Fig.2 we see the optimal impact leading to the melting of the outer polymer shell and creation of fused droplets on the substrate, formed after cooling of the hemisphere with the characteristic radius, depending on the temporal and energy parameters of the laser radiation. At the same time, in the right top part of Fig. 2 we observe the exit beyond the region of optimal laser irradiation that leads to the destruction of the central part and disappearance of luminescence from the central part of the droplets, which corresponds to the destruction of the sensitive elements. One can draw a diagonal from the left top corner of Fig. 2 to the right bottom one, dividing it into two regions, namely, the region of the destroyed sensitive elements and the region of central parts efficiently interacting with the luminophore.

To increase the laser fused deposition density we studied the impact of the laser radiation with small (3 μm) diameter of the laser spot, comparable with the diameter of the polymer microparticles (3–4 μm). However, the consideration of the theoretical model, describing the influence of thermoplasticity on the maximal deposition density, has shown that it is not reasonable to decrease the laser spot diameter below 6 μm, since the large temperature gradients arising in this case and the corresponding plastic deformations (10) increase the diameter of the element, produced by laser fused deposition, thus decreasing the deposition density.

The developed theory allowed the choice of laser irradiation parameters, close to the optimal ones (the laser radiation wavelength 532 nm, the power 40 mW, the time of impact 10 ms, the diameter of the focal spot 6 μm) and the conduction of laser irradiation providing a high density of the deposited elements. With respect to the power density this corresponds to the central part of the data range, presented in Fig. 2 (the spot diameters 15 μm, the power 250 mW, the pulse duration 10 ms). In this experiment in the case of small laser spot the diameter of the fused droplets amounted to 13–14 μm, the grain of the polymer film being 3–4 μm. The fluctuation of the droplet diameter can be due to the nonuniformity of the grain of the polymer microparticles layer. The reached density of deposition in this case is 110000 spots per 1 cm^2.

In comparison with the first series of experiments (with the laser spot diameter 15 μm) the reduction of the spot diameter by 2.5 times (to 6 μm) allowed the reduction of the laser fused zone by 2.2 times (to 13.5 μm), the laser pulse duration being 10 ms. The reduction of the separation between the droplets is limited not only by the diameter of the laser melted zone, but also by the distance of heat transfer, depending on the pulse duration, and the heat conductivity coefficient of the polymer matrix, enclosing the graphite nanoparticles. For the considered system, the minimal possible separation between the fused droplets is nearly 20 μm, which allows the deposition density up to 250000 spots per 1 cm^2.

8. Conclusions

The theoretical model of the process of laser melting of the layer of polymer microparticles with an embedded sensitive element allows the assessment of the conditions of thermal and thermomechanical damage of sensitive elements. For the first time the boundaries of the acceptable ranges and the optimal values of the laser parameters that provide the polymer shell melting without the damage of the sensitive element of the biochip are theoretically determined. It is shown that the reduction of the laser spot diameter and the laser pulse duration is reasonable up to certain limits determined by the processes of heat conduction and thermoplasticity of the polymer matrix, as well as by the mechanism of thermomechanical destruction of the sensitive element. The experimen-

tal study of the influence of the power, laser spot diameter, and laser pulse duration on the size of the fused droplet confirmed the results and conclusions of the developed theory. For the diameter of the laser spot 6 μm and the pulse duration 10 ms the fused elements with the diameter 13.5 μm were obtained, the corresponding deposition density being 110000 spots per 1 cm^2. The maximal possible densities of laser fused deposition for this system were estimated to be 250000 spots per 1 cm^2.

Acknowledgements. A few of stages of this work were carried out under the support from the Russian Foundation for Basic Research (Grant Nos 12-02-91326-SIG_a/HRGRG-316, 15-02-06078_a and 14-02-90005 Bel_a).

References

1. Angenedt P. *Drug Discovery Today*, **10**, 503 (2005).
2. Chang T.W. *J. Immunol. Meth.*, **65**, 217 (1983).
3. MacBeath G., Schreiber S. *Science*, **289** (5485), 1760 (2000).
4. Kulesh D.A., Clive D.R., Zarlenga D.S., Greene J.J. *Proc. Natl. Acad. Sci. USA*, **84**, 8453 (1987).
5. Lashkari D.A., DeRisi J.L., McCusker J.H., Namath A.F., Gentile C., Hwang S.Y., Brown P.O., Davis R.W. *Proc. Natl. Acad. Sci. USA*, **94**, 13057 (1997).
6. *Reviews: The Chipping Forecast. Nature Genetics*, **21** (1999).
7. Vasiliskov V., Tirnofeev E., Surzhikov S., Drobyshev A., Shick V., Mirzabekov A. *BioTechnique*, **27**, 592 (1999).
8. Bavykin S.G., Akowski J.P., Zakhariev V.M., Barsky V.E., Mirzahekov A.D. *Appl. Environ. Microbiol.*, **67**, 922 (1997).
9. Chechetkin V.R., Turygin A.Y., Proudnikov D.Y., Prokopenko D.V., Kirillov Eu.V., Mirzabekov A.D. *J. Biomol. Struct. Dyn.*, **18**, 83 (2000).
10. Elcins R.P. *Clin. Biochem. Revs.*, **8**, 1222 (1987).
11. Elcins R.P., Berger H., Chu F.W., Finckh P., Krause F. *Nanobilogy*, **4**, 197 (1998).
12. Elckins R.P., Chu F.W. *Clin. Chem.*, **37**, 1955 (1991).
13. Schirwitz C. *Springer International Publishing Switzerland*, doi 10.1007/978-3-319-00807-3, ISBN: 978-3-319-00806-6 (Print), 978-3-319-00807-3 (Online) (2013).
14. Sobol E.N., Milner T.E., Shekhter A.B., Baum O.I., Guller A.E., Ignatieva N.Y., Omelchenko A.I., Zakharkina O.L. *Laser Phys. Lett.*, **4** (7), 488 (2007).
15. Stadler V., Felgenhauer T., Beyer M., Fernandez S., Leibe K., Guttler S., Gruning M., Kunig K., Torralba G., Hausmann M., Lindenstruth V., Nesterov A., Block I., Pipkorn R., Poustka A., Bischof F.R., Breitling F. *Angew. Chem. Int. Ed.*, **47**, 7132 (2008).
16. Baum O.I., Shcherbakov E.M., Minaeva S.A., Nesterov-Müller A., Merkle F., Sobol' E.N. *Izv. Ross. Akad. Nauk, Ser. Fiz.* (to be published).
17. Sobol E. *Phase Transformations and Ablation in Laser-Treated Solids* (New York: John Wiley & Sons Inc., 1995).
18. Timoshenko S., Goodier J.N. *Theory of Elasticity* (New York : McGraw-Hill, 1970; Mscow: Nauka, 1975).
19. Beyer M., Nesterov A., Block I., Kunig K., Felgenhauer T., Fernandez S., Leibe K., Torralba G., Hausmann M., Trunk U., Lindenstruth V., Bischoff F.R., Stadler V., Breitling F. *Science*, **318**, 1888 (2007).
20. Grigoriev I.S., Meilikhov E.Z. (Eds) *Handbook of Physical Quantities* (Boca Raton, NY: CRC Press, 1996; Moscow: Energoatomizdat, 1991).
21. Ishlinskii A.Yu., Ivlev D.D. *Matematichskaya teoriya plastichnosti* (Mathematical Theory of Plasticity) (Moscow: Fizmatlit, 2001).
22. Bowden P.B. *Phil. Mag.*, **29**, 149 (1974).